

ultraharmonic response may be equally treated by our method after small alternations in its process. But all these are left for future study.

6. Acknowledgement

The author expresses his sincere thanks to Prof. S. Fujii and Mr. H. Sato of Tokyo University for encouragements and conveniences given to him, especially in the analog computer experiment.

References

- (1) S. Maezawa : *Proc. 9th Japan Nat. Congr. Appl. Mech.* 1959, (1960), p. 319.
- (2) S. Maezawa : *Bulletin of JSME*, Vol. 4, No. 14, (1961), p.201.
- (3) S. Maezawa : *Proc. 10th Japan Nat. Congr. Appl. Mech.* 1960, (1961), p.405.
- (4) S. Maezawa : *Reports of the Faculty of Engineering Yamanashi University*, Vol. 11 (1960), p. 26.
- (5) S. Maezawa : *Reports of the Faculty of Engineering Yamanashi University*, Vol. 10 (1959), p. 28.
- (6) Numerical tables for these coefficients are included in (4), which are available on request.
- (7) J.G. Truxal : *Control System Synthesis* (1955), chap. 10, McGraw-Hill.

531. 717. 082. 36:532. 525

Action of the Fluid in the Air-Micrometer*

(1st Report, Characteristics of Small-Diameter Nozzle and Orifice No. 1, In the Case of Compressibility Being Ignored)

By Yasutoshi NAKAYAMA**

Using 5 types of rounded nozzles, 24 types of cylindrical nozzles ($l/d=0.799\sim 16.520$, l : length, d : diameter) and 5 types of knife-edged orifices of 0.3 mm to 1.2 mm diameter, the discharge characteristics were investigated for Reynolds number from 550 to 10 000, using distilled water and low-pressure air.

The results are summarized :

1. Discharge coefficients, which were calculated on the basis of experiments using distilled water and low-pressure air, fall on the same curves, if arranged by Reynolds number and l/d .
2. Discharge coefficients for each type of nozzle or orifice were collected and one experimental formula was worked out.
3. Downstream pressure of nozzle or orifice is reduced to a minimum at a position of about 1.2 times the pipe diameter and is recovered at about 5 times the pipe diameter.
4. Recovery rate of pressure is about $1.7m$ (m : area ratio) for rounded nozzles and $1.2m$ for others.

1. Introduction

The measurement based on the theory of so-called air-micrometer is not only applied to that of precise dimensions, but also to the strain-meter, roughness meter, dynamometer, tachometer, and further the utilization of this method covers a very wide field including automatic gaging, automatic control system, etc. For measuring, as shown in Fig. 1, two nozzles are used, namely, a nozzle B, which is changed by

an object C, and a nozzle A, which is for measurement of the discharge quantities from the nozzle B, and the indicating pressure between two nozzles, p_2 , is used for measurement. It is the two nozzles that determine the indicating pressure exactly, and

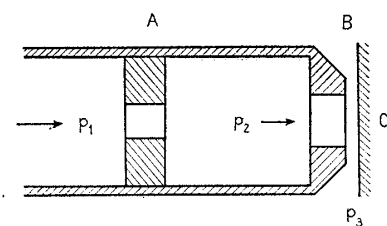


Fig. 1 Schematic diagram of air-micrometer

* Received 9th May, 1960.

** Chief Research Engineer, Railway Technical Research Institute, Japanese National Railways, Kokubunji, Tokyo.

in order to obtain the characteristic equation precisely, discharge coefficients of the two nozzles have to be known accurately.

In the sense mentioned above, these studies which will be reported in due course, have been carried out for the following purpose ; to clarify the characteristics of the two nozzles, to obtain exact characteristic equations which are suitable to actual installations, to establish the method by which gaging instruments using a fluid can be designed correctly, and to improve the accuracy of the instruments.

In the case of pressure type or vacuum type, commonly small diameter orifices and nozzles are used for throat A about 0.3 to 1.2 mm in diameter. Up to date, concerning the throat for air-micrometer, there are several reports in which the discharge coefficient was calculated for the testing of low pressure air indicating 500 mmAq for pressure difference^{(1)~(3)}, but influences of the measuring conditions, such as type of throat, opening ratio, diameter, length, pressure measuring position and Reynolds number on the discharge coefficient have not been investigated in detail.

As to studies of nozzles and orifices for common uses, many of them have been carried out with the object of measuring discharge quantities by the standard type of them, and studies about the following discharge coefficients for such nozzles and orifices are well established ; namely, Reynolds number more than 10 000, diameter of pipe above 50 mm and opening ratio above 0.05^{(4)~(7)}. On the contrary we are able to find only a few studies on nozzles and orifices for measurement of small discharge quantities, in which such nozzles and orifices having less diameter and lower Reynolds number are investigated^{(8)~(12)}. Especially we have less studies on cylindrical nozzles^{(11)~(12)}.

Moreover, it is much more difficult to find any study on the throat which is less than 1 mm in diameter and is suitable for the air-micrometer^{(9)~(11)}. The results of such study, if any, will not be applicable to the air-micrometer because of the difference in ranges, conditions and the purpose of study.

In this report, the discharge characteristics of 34 types of nozzles and orifices which vary from 0.3 to 1.2 mm in inner diameter were investigated for Reynolds number from 550 to 10 000 using distilled water and dry air which has pressure up to 600 mmAq and for which the compressibility can be ignored. The results of this study will be applicable directly in calculating the characteristics of low pressure type air-micrometer and liquid-micrometer, and also in measuring smaller discharge quantities

or in designing a throat for automatic control, shock absorber and damper.

2. Nomenclature

The following nomenclature is used in this paper :

- G : rate of weight flow
- Q : rate of volume flow
- c : discharge coefficient
- c_c : contraction coefficient
- c_v : velocity coefficient
- ζ : head loss coefficient
- p_1 : pressure just before the throat (absolute pressure)
- p_2 : pressure just after the throat (absolute pressure)
- $p_m = (p_1 + p_2)/2$: mean pressure
- γ : specific weight of fluid
- γ_w : specific weight of water
- γ_a : specific weight of air
- γ_{am} : specific weight of air for p_m
- t : temperature of fluid
- v : mean velocity of fluid passing through throat
- μ : coefficient of absolute viscosity of fluid
- ν : coefficient of kinematic viscosity of fluid
- g : acceleration of gravity
- d : throat diameter
- D : pipe diameter
- l : throat length
- a : area of throat cross section
- $m = (d/D)^2$: opening ratio

3. Measuring room

The experiments described in the following were performed in a constant temperature and humidity room. (temperature $20 \pm 0.5^\circ\text{C}$, humidity 65%).

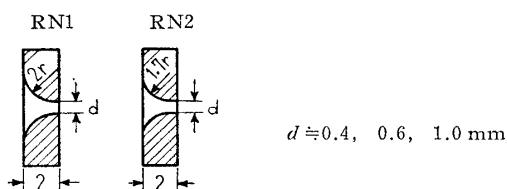
4. Throat used for experiments

As shown in Fig. 2, these experiments are carried out on 34 types of nozzles and orifices including 5 types of rounded nozzles, 24 types of cylindrical nozzles and 5 types of knife-edged orifices. These nozzles and orifices are made accurately of brass on the lathe for clocks, and cut to desired length after drilling holes to eliminate the difference in diameters of entrance and center. Thereafter, they were lapped on both sides and bores. The bores were measured very carefully in regard to two directions at right angles by a comparator (accuracy 1μ) and remade again and again if the difference between them was large. As a result, the deviations from mean value of diameter at every nozzle and orifice did not exceed 1.3% and in general were less

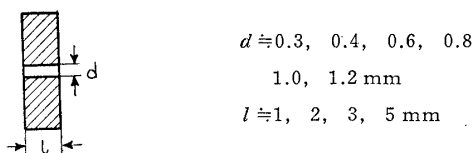
than 0.8%, and the deviations from mean value of diameter of both sides in a cylindrical nozzle were less than 0.5%. Thus ellipticity and conicality of

Table 1 Throat used for experiments

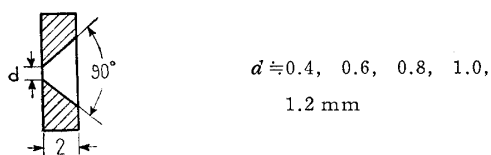
Type and number	Diam. d mm	Length l mm	l/d	Pipe diam. D mm	Opening ratio $m=(d/D)^2$	
Rounded nozzle	RN1-1	0.610		6.29	0.0094	
	2	1.045		"	0.0276	
	RN2-1	0.405		"	0.0042	
	2	0.609		"	0.0094	
	3	0.994		"	0.0250	
	Cylindrical nozzle	CN1-1	0.314	1.009	3.213	0.0025
2		0.434	1.010	2.327	0.0047	
3		0.637	0.954	1.498	0.0102	
4		0.801	1.015	1.267	0.0161	
5		1.004	0.948	0.944	0.0253	
6		1.208	0.965	0.799	0.0367	
CN2-1		0.302	2.030	6.722	6.29	0.0023
2		0.420	2.015	4.804	"	0.0045
3		0.631	2.004	3.174	"	0.0101
4		0.806	2.009	2.493	"	0.0165
5		1.002	2.015	2.011	"	0.0254
6		1.202	2.011	1.673	"	0.0365
CN3-1		0.290	2.989	10.307	6.33	0.0021
2		0.449	2.996	6.673	"	0.0050
3		0.619	3.001	4.848	"	0.0096
4		0.805	3.026	3.759	"	0.0162
5		1.007	2.994	2.973	"	0.0253
6		1.210	2.968	2.453	"	0.0366
CN4-1		0.301	4.973	16.520	6.36	0.0022
2		0.402	4.977	12.381	"	0.0040
3		0.622	4.991	8.024	"	0.0096
4		0.808	5.026	6.220	"	0.0162
5		1.011	4.979	4.925	"	0.0253
6		1.203	4.993	4.151	"	0.0358
Knife-edged orifice	KO-1	0.434		6.29	0.0048	
	2	0.617		"	0.0096	
	3	0.801		"	0.0162	
	4	1.007		"	0.0256	
	5	1.206		"	0.0368	



Rounded nozzle (RN)



Cylindrical nozzle (CN)



Knife-edged orifice

Fig. 2 Throat used for experiments

the throats were so little that the area of discharge was computed using mean values of diameter as shown in Table 1.

5. Pipe with a throat

As shown in Fig. 3, nozzles and orifices were installed in acryl resin pipes of inside diameter 6 mm and outside diameter 12 mm and with an acryl resin flange on one side. The surface of these pipes was very smooth with excellent roundness, but with different diameters, so several pipes, of which the deviations from mean value of diameter were less than 1%, were picked up from among several hundred pipes at plants and used for experiments. The diameters of these pipes are shown in Table 1. As shown in Fig. 3 and Table 2, 11 pressure taps (diameter 0.3 mm) were set up upstream and 16 downstream, and connected to the manometer with vinyl pipes having inside diameter 3 mm.

And at the position of pressure taps Nos. 1, 6, 17, 24, 27 the thermocouples consisting of copper (0.2 mmφ) and constantan (0.15 mmφ) were installed. These positions of temperature measurement were named e, f, g, h, i as shown in Fig. 3. At e, f the thermocouples were set in the direction of diameter to measure the temperature at the center of fluid

Table 2 Position of pressure tap

Pressure tap No.	Position L_1 mm	Pressure tap No.	Position L_2 mm
1	600	12	1
2	360	13	1.5
3	180	14	3
4	60	15	4.5
5	18	16	6
6	12	17	9
7	9	18	12
8	6	19	15
9	4.5	20	18
10	3	21	24
11	1	22	30
		23	36
		24	42
		25	60
		26	120
		27	180

L_1 : Distance upstream from throat front
 L_2 : Distance downstream from throat back

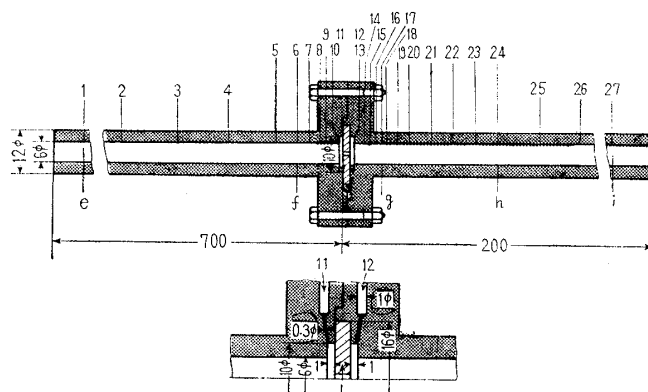


Fig. 3 Throat-installed pipe

flow but at the other positions they were set with the tip projecting 0.3 mm from the internal wall of the pipe to measure the temperature of fluid.

For installation of nozzle and orifice, mylar (thickness 0.02 mm) was used as packing material.

6. Experimental apparatus and method

6.1 Experiment using distilled water

The experimental apparatus is represented in Fig. 4. The distilled water which is held in the water tank ① (volume 75 l) is sent by the gear pump ② to the constant head device ④ through «Ever Last» metallic filter ③* and the water which attains a constant head here is sent to the throat-installed pipe ⑦ through a 12 mm vinyl pipe ⑤ running through valve ⑥. Valve ⑧ was set to exert all the time a little pressure downstream of the throat. The pressure distribution upstream and downstream of the throat was measured using a 6 mm gage-glass manometer ⑨. The deviation from mean value of inner-diameter of these gage-glass pipes did not exceed 2.5%. If d_g is inner-diameter of the pipe, the height h of rising water level in the pipe by capillary action is $30/d_g$ (where h , d_g measured in mm)⁽¹³⁾, so the error of indicating pressure is ± 0.1 mm maximum.

Following the German standards the desired pressures just before and after the test nozzle and orifice, p_1 and p_2 , were regulated exactly by the pressure of Nos. 11, 12 taps. The experiments were conducted up to the head of 3 m. About the throats of 0.3, 0.4 mm diameter, experiments were conducted up to the head of 23 m by applying a direct water pressure by means of a gear-pump.

A thermocouple and a milli-voltmeter (2 mV) were used to measure the temperature at each point upstream and downstream of the nozzle and orifice.

6.2 Experiment using low pressure air

The experimental apparatus is represented in Fig. 5. The compressed air was sent to the throat-installed pipe passing through the coil hose ② which is in the water-tank ① (20°C), the filters ③, ⑤, the dehydrater ④ (the air drying apparatus using silica gel), the automatic pressure regulator ⑥, the fine adjustable valve ⑦, «Ever Last» metallic filter ⑧ (clearance 2μ). The air coming out of the throat-installed pipe was collected in a messcylinder ⑪ which is placed upside down in the water-tank ⑩ and the flow quantities were measured. The pressure distribution upstream and downstream of the throat

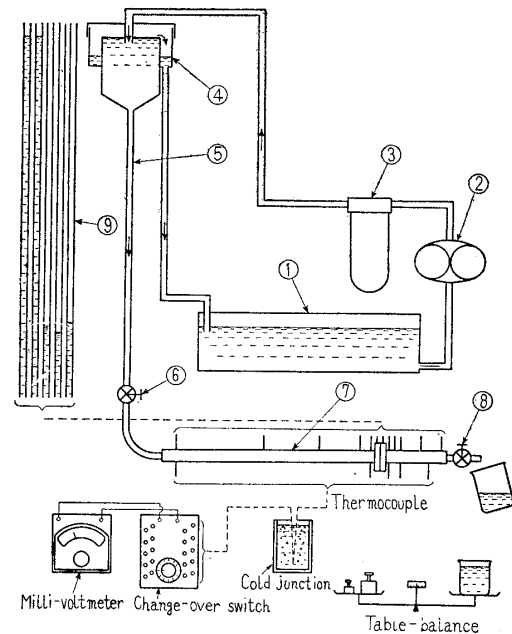


Fig. 4 Experimental apparatus (for distilled water)

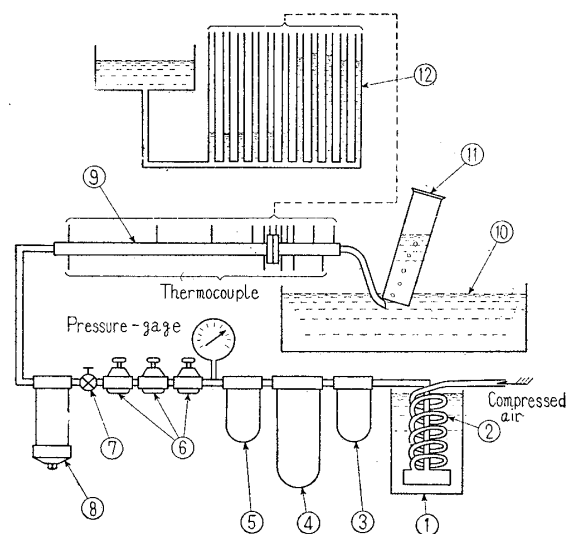


Fig. 5 Experimental apparatus (for low pressure air)

was measured using a water manometer ⑫ (inner diameter 10 mm gage-glass pipes). By means of the fine adjustable valve ⑦, p_1 and p_2 were obtained exactly by the pressure of Nos. 11, 12 taps as in the case of distilled water. The experiments were conducted up to 600 mmAq. The difference in water level owing to the irregularity of inside diameter of manometer glass pipe was 0.1 mm maximum. The humidity of air passing through nozzle and orifice was measured by Minima Sensible Hygrometer⁽¹⁴⁾ and the value was less than 10%, so this air can be treated as dry air.

* The element of this filter is made of sintered spherical metallic particles and the clearance between particles is 5μ .

7. Arrangement methods of experimental results

The flow quantities of an incompressible fluid passing through the throat in unit time are represented by next equation.

$$Q = ca \sqrt{\frac{2g(p_1 - p_2)}{\gamma}} \dots\dots\dots (1)$$

In the case of low pressure air, γ_{am} is used. The discharge coefficient must be determined experimentally. In the case of this experiment the nozzle and orifice are so-called submerged orifice so there can be no effect from surface tension⁽¹⁵⁾. So c is seemingly found to be a function of $\gamma, \mu, \nu, (p_1 - p_2), D, d, l$. Thus five non-dimensional products are obtained from π theorem. Namely,

$$c = \varphi \left\{ \frac{vd}{\nu}, \frac{l}{d}, \frac{d}{D}, \frac{(p_1 - p_2)}{\gamma d} \right\} \dots\dots\dots (2)$$

d/D affects c as increasing velocity of approach, and the magnitude of it is represented by $1/\sqrt{1 - c_e^2 m^2}$ ⁽¹⁶⁾. In the case of this experiment, the maximum value of m is 0.04, so there is no influence of d/D . And there is little effect from $(p_1 - p_2)/\gamma d$ in this experiment. So excepting these terms, next equation is obtained.

$$c = f \left(\frac{vd}{\nu}, \frac{l}{d} \right) = f \left(R_e, \frac{l}{d} \right) \dots\dots\dots (3)$$

In the case of this experiment, c is obtained from Eq. (1), and the results are arranged by Eq. (3). And $R_e = d\sqrt{2g(p_1 - p_2)}/\gamma/\nu$ was used as Reynolds number for the convenience of computation.

In the case of low pressure air, if Q represents the volumetric rate of flow measured by messcylinder, γ_a the specific weight of it, Eq. (1) will become,

$$Q \frac{\gamma_a}{\gamma_{am}} = ca \sqrt{\frac{2g(p_1 - p_2)}{\gamma_{am}}} \dots\dots\dots (4)$$

As stated before, the air passing through the throat can be regarded as dry air, so the computation of γ_{am} was done by the next equation.

$$\gamma_{am} = 1.2931 \times \frac{273}{273 + t_1} \times \frac{h_m}{760} \text{ kg/m}^3 \dots\dots\dots (5)$$

t_1 is the temperature °C of the air upstream, h_m is the height of mercury column mm of p_m at 0°C.

The air in the messcylinder was regarded as saturated air and γ_a was determined from the next equation using $h_3 - \varphi F$ instead of h_m in Eq. (5).

$$\gamma_a = 1.2931 \times \frac{273}{273 + t_3} \times \frac{h_3 - \varphi F}{760} \text{ kg/m}^3 \dots\dots\dots (6)$$

Here, t_3 is the temperature °C of the air in the messcylinder, h_3 is the atmospheric pressure mmHg (converted into the value of 0°C), φ is the relative humidity (asumed as 1 here), F is the pressure of saturated steam mmHg⁽¹⁷⁾ at t_3 °C.

8. Results and considerations

8.1 Discharge coefficient

8.1.1 Rounded nozzle From experimental results, c versus R_e curve was plotted as in Fig. 6. According as Reynolds number increases, c approaches a constant value, but within the range of experiments c is still in the trend to increase. From Fig. 6, Eq. (7) is obtained as an experimental formula

$$c = 0.589 R_e^{0.05} \dots\dots\dots (7)$$

In the range of $800 < R_e < 8000$, the deviation of the measured from this experimental formula is about 3% maximum.

8.1.2 Cylindrical nozzle From the experimental results, the relation c versus $\log R_e$ taking parameter l/d is shown in Fig. 7. According as Reynolds number increases, c becomes or approaches a constant value. A plot of this value of versus l/d is shown in Fig. 8. Because there are no other data for the cylindrical nozzles of small diameter, the experimental results of W. Könncke⁽¹⁸⁾ and A. L. Jorissen and H. T. Newton⁽¹⁹⁾ which are in some degree larger in diameter are shown in this figure. From Fig. 8, in the case of the value of l/d being small, the discharge coefficients increase rapidly with an increasing l/d , and c becomes 0.817 in the neighborhood of $l/d = 1.5$, and with an increasing l/d , c decreases gradually. But in the case of $l/d = 0.799$

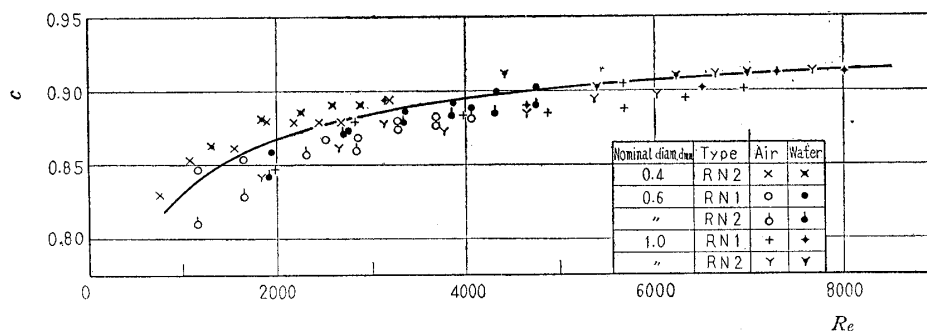


Fig. 6 Discharge coefficient of cylindrical nozzle

($d \doteq 1.2$ mm, $l \doteq 1$ mm), $l/d = 0.944$ ($d \doteq 1$ mm, $l \doteq 1$ mm), the discharge coefficient was divided in two kinds in water and became unsteady, but in the air such phenomenon was not seen.

From Fig. 8, Eq. (8) was obtained at $1.5 < l/d < 17$.

$$c = 0.868 - 0.0425(l/d)^{1/2} \dots\dots\dots(8)$$

The deviation of the measured value from this experimental formula is less than 1%.

If the range of Eq. (8) is approximated by a straight line, Eq. (9) is obtained. If this equation is used, the error will be within 1.5%.

$$c = 0.819 - 0.00791l/d \dots\dots\dots(9)$$

Next, let us consider the region in which c shown in Fig. 7 changes in a great measure with R_e and l/d . According as R_e becomes small the phenomenon of contraction becomes less conspicuous and the values of c that are arranged like Fig. 8 at the place of large R_e will be arranged all in the order of l/d at $R_e < 1000$.

Now, an experimental formula is induced about the range of $1.5 < l/d < 17$. From the relation of $\zeta = \{(p_1 - p_2)/\gamma\} / (v^2/2g) = 1/c^2$, the data of l/d versus

$\sqrt{\zeta \cdot R_e}$ where R_e is parameter are represented by the following Eq. (10),

$$\sqrt{\zeta \cdot R_e} = A(l/d) + B \dots\dots\dots(10)$$

When A or B is determined from the relation of R_e , Eq. (11) is obtained. And Eq. (12) is obtained from Eq. (11)

$$\sqrt{\zeta \cdot R_e} = \frac{17.11}{R_e^{1/3}} \frac{l}{d} + 1.65 R_e^{2.8/6} \dots\dots\dots(11)$$

$$c = \frac{R_e^{5/6}}{17.11l/d + 1.65 R_e^{4.8/6}} \dots\dots\dots(12)$$

Comparing the values of c from Eq. (12) with the experimental values and plotting main values of them, Fig. 9 is obtained. In the region of $1.5 < l/d < 17$, $550 < R_e < 7000$, the error is 2.8% maximum, being mostly within 2%.

Next, putting $R_e = 7000$ in the right side of Eq. (12) and computing c , the values of Eq. (12) are well continuous from Eq. (8) or Eq. (9).

8.1.3 Knife-edged orifice From experimental results, the relation of c versus R_e is shown in Fig. 10; c becomes constant at 0.63 near $R_e = 5000$. As the diameter of these orifices is small, the value

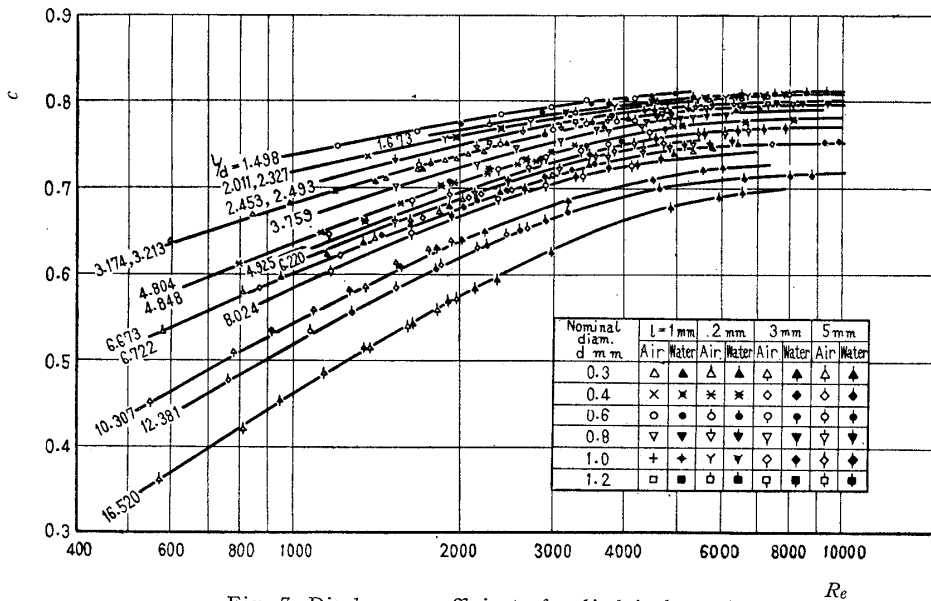


Fig. 7 Discharge coefficient of cylindrical nozzle

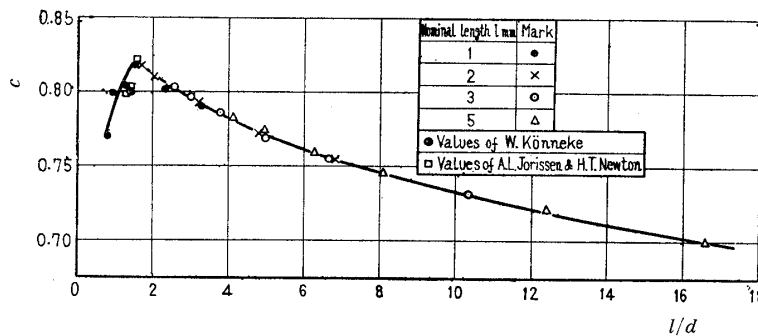


Fig. 8 Relation of c versus l/d over so-called "limit of constancy" of Reynolds number

of 0.63 is larger than the final Reynolds number $c=0.593$ of standard orifice⁽²⁰⁾. From Fig. 10, the experimental formula (13) is obtained for $800 < R_e < 5000$.

$$c = \frac{0.964}{R_e^{0.05}} \dots \dots \dots (13)$$

The deviation of the measured value from this experimental formula is about 2%.

8.2 Pressure distribution

In the upstream side of the throat, there is no difference of pressure. One example of the pressure distribution in downstream of the throat is shown in Fig. 11. The pressure distribution becomes minimum at the place of about 1.2 times the pipe diameter from the downstream side of the throat, and recovers at 5 times that diameter. The recovery rate of pressure (ratio of recovered pressure to differential pressure) is to be determined from the type of throat; for a rounded nozzle it is about 1.7m, $[m = (d/D)^2]$, for a knife-edged orifice about 1.2m, and in the case of a cylindrical nozzle about 1.3m, 1.2m and 1.0m for the values of l are 1 or 2 mm, 3 mm and 5 mm respectively.

8.3 Influence of position of pressure tap on c

Putting p_2' as the recovered pressure, from the preceding statement, we have,

$$p_2' = p_2 + bm(p_1 - p_2)$$

Therefore

$$p_1 - p_2 = \frac{p_1 - p_2'}{1 - bm} \dots \dots \dots (14)$$

Here, b is constant and it may be considered to be 1.7 for a rounded nozzle and 1.2 for the other types. So when the pressure taps were located at more than 5 times the pipe diameter from the downstream side of the throat, computation may be made by substituting Eq. (14) into Eq. (1). But the error of c calculated from Eq. (1) is 1/2 as large as the error of differential pressure, so if the error of c permitted up to 1%, from the preceding statement the position of pressure taps need not be considered till $m=0.02$, say, for cylindrical nozzle.

8.4 Loss in inlet region

About the cylindrical nozzle let us consider the loss in the inlet region. Since $c=f(R_e, l/d)$ from $\zeta = \{(p_1 - p_2)/\gamma\} / (v^2/2g) = 1/c^2$, so $\zeta = \varphi(R_e, l/d)$.

About the pressure loss P_f by Poiseuille viscosity loss, there is $(P_f/\gamma) / (v^2/2g) = 64/R_e \cdot l/d$. Now computing ζ using the measured values, put the coefficient of additional loss of head which is obtained by subtracting $(P_f/\gamma) / (v^2/2g)$ from ζ , as ξ , then the relation of ξ versus $l/(d \cdot R_e)$ in the region of laminar flow ($cR_e < 2300$, but $R_e = d\sqrt{2g(p_1 - p_2)/\gamma}/\nu$) will be as shown in Fig. 12; ξ is an energy loss occurring in the change from pressure energy to velocity energy and is equal to the sum of excess energy loss for the change of velocity distribution and inlet energy loss. The dotted line and full line in the same diagram show respectively the theoretical value according to Schiller⁽²¹⁾ and Atkinson and Goldstein⁽²²⁾. As long as the value of $l/(d \cdot R_e)$

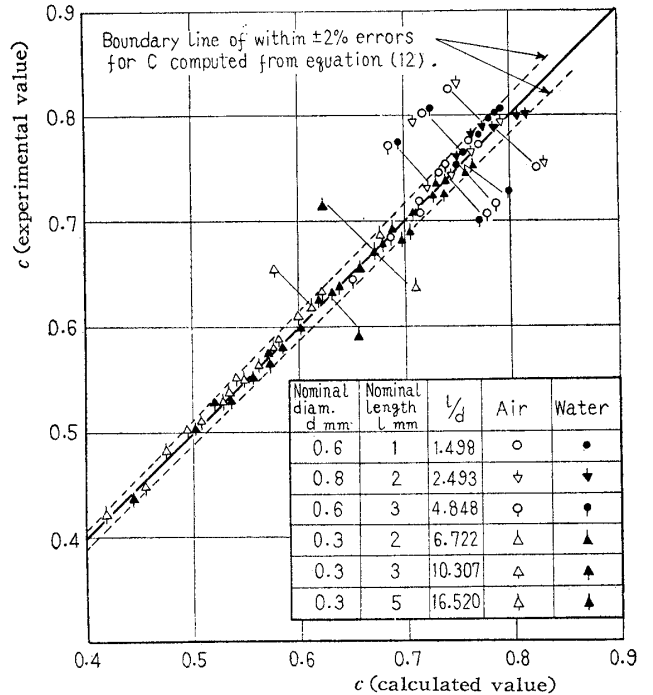


Fig. 9 Comparison of calculated values from experimental formula with experimental values of discharge coefficient of cylindrical nozzle

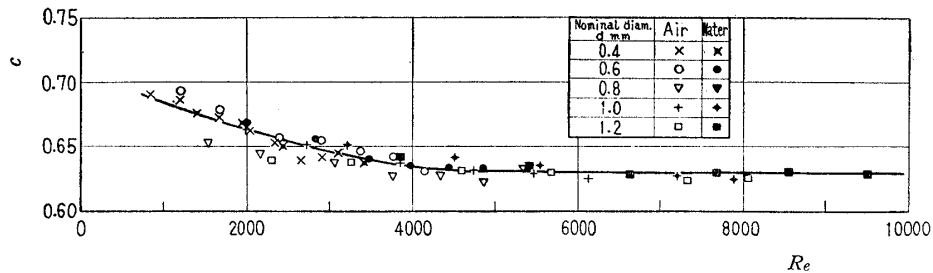


Fig. 10 Discharge coefficient of knife-edged orifice

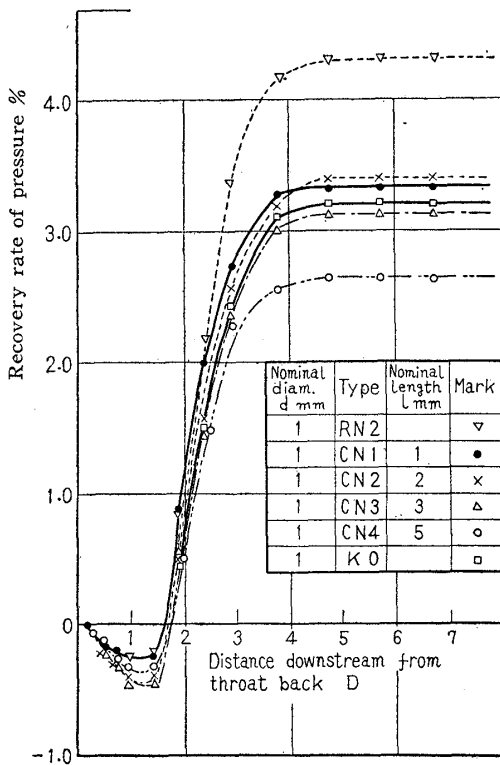


Fig. 11 Pressure distribution at pipe wall downstream of throat

is small, the loss is larger than the theoretical value of Schiller. This is presumably due to the fact that in the case where l/d is small or Re is large, the velocity energy changing just after the inlet is larger than the energy assumed on the condition that the velocity distribution of inlet is uniform.

If $l/(d \cdot Re)$ becomes larger than about 0.01, it approaches the theoretical value of Atkinson and Goldstein but becomes a little small value, and approaches 2.36 which becomes constant at $l/(d \cdot Re) > 0.063$ in the case of the earlier experiments⁽²³⁾ on copper capillary. Thus, the fact that the experimental value using the pipe having a non-rounded entrance is equal to the theoretical value considering the uniform velocity distribution at entrance, is presumably due to the fact that in the pipe having a non-rounded entrance the laminar flow loss for the fluid to approach the entrance cancels the decrease in pressure loss of viscosity by exfoliation⁽²⁴⁾; the velocity energy increases just after the inlet owing to contraction, but excessive energy consumed for the change of velocity distribution in the inlet region is not so different from the theoretical value calculated on the assumption that the velocity distribution of entrance is uniform.

Further, in the case of turbulent flow, experimental values deviate from these curves.

8.5 Region available for air-micrometer

In the region of the ratio of indicating pressure

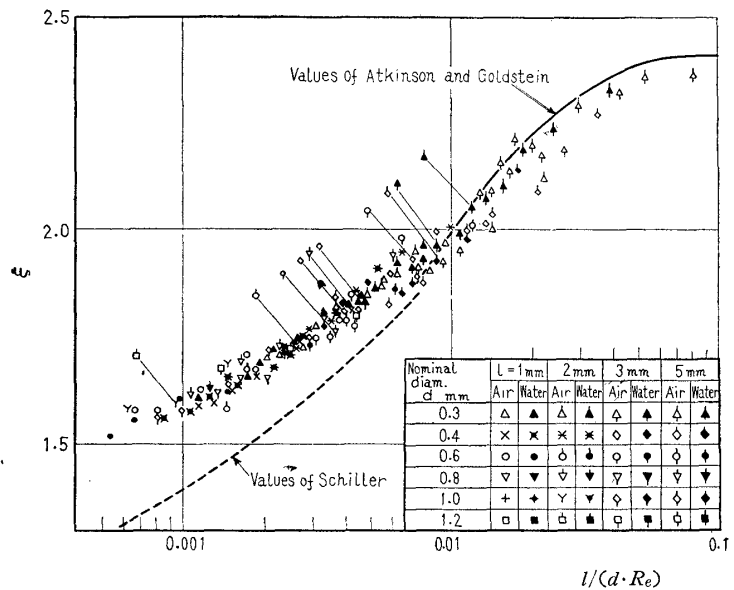


Fig. 12 Additional loss of head coefficient of inlet region

and initial pressure being 0.4 to 0.9, the characteristic of air-micrometer shows approximately a linear relation. This region corresponds to 200 to 450 mmAq in the 500 mm water-column type air-micrometer and using a throat with diameter 0.3 to 1.2 mm, the Reynolds number becomes about 1 000 to 7 000. So it is understood that the discharge coefficient which is assumed constant up to now changes in a considerably wide range.

9. Conclusion

In regard to the throat of air-micrometer, a precision test was done using distilled water and low pressure air, and the characteristic of throat was made clear as follows :

(1) Discharge coefficients, which were calculated on the basis of experiments using distilled water and low-pressure air, fall on the same curves, if arranged by Reynolds number and l/d .

(2) Discharge coefficients of each type of nozzle and orifice have been able to be expressed by respective experimental formulas.

(3) Downstream pressure of nozzle or orifice is recovered at about 5 times the pipe diameter and the recovery rate of pressure is determined depending on the type of throat.

(4) The loss in inlet region of cylindrical nozzle is made clear.

(5) About the small diameter nozzle, a cylindrical nozzle is easy to make, has high reliability of discharge coefficient, and has superior characteristics. But in the case of using a fluid, it is inadequate to use the nozzle of $l/d < 1.3$ owing to the unstable discharge coefficient.

Acknowledgement

The author wishes to express cordial appreciation to Prof. Emeritus I. Oki Waseda University, Prof. S. Iwanami Tokyo Metropolitan University and head of his laboratory Mr. R. Nakamura for their kind advices and suggestions. At the same time he is grateful to Mr. H. Endo in his laboratory and Mr. H. Miura a student of Chiba Technical College at that time for their assistance in the experimental work and data arrangement.

References

- (1) S. Ishiwara: *Jour. Soc. Prec. Mech. Japan*, Vol.13, No. 10-11-12 (1947), p. 80.
- (2) Y. Ueoka: *Technical Report of Yamaguchi University*, Vol. 2, No. 1 (1951), p. 45.
- (3) A. Kobayashi: *Journal of Electrical Laboratory*, Vol. 16, No. 12 (1952), p. 946.
- (4) *Regeln für die Durchflussmessung mit genormten Düsen, Blenden und Venturidüsen*, DIN (1952).
- (5) *Fluid Meters, Their Theory and Application*, Report of the ASME Special Research Committee on Fluid Meters, 4th Edition, (1937).
- (6) *Flow Measurement*, British Standard Code, B. S. 1042, (1943).
- (7) JIS B 8302 (1954).
- (8) H.R. Linden and D.F. Othmer: *Trans. ASME*, Vol. 71, No. 7 (1949), p. 765.
- (9) H.P. Grace and C.E. Lapple: *Trans. ASME*, Vol. 73, No. 5 (1951), p. 639.
- (10) H.W. Iversen: *Trans. ASME*, Vol. 78, No. 2(1956), p. 359.
- (11) S. Iwanami: *Trans. Japan Soc. Mech. Engrs.*, Vol. 18, No. 66 (1952), p. 52.
- (12) T. Tanaka: *Trans. Japan Soc. Mech. Engrs.*, Vol. 19, No. 85 (1953), p. 107.
- (13) I. Oki: *SUIRIKI GAKU(Hydraulics)* (1948), p. 20, Iwanami Shoten.
- (14) K. Shiba: *High Polymer*, Vol.7, No. 70(1958), p. 72.
- (15) S. Itaya: *SUIRIKI GAKU (Hydraulics)*, (1959), p. 85, Japan Soc. Mech. Engrs.
- (16) *ibid.* (13), p. 99.
- (17) *The Steam Tables and Diagrams*, (1950), Japan Soc. Mech. Engrs.
- (18) W. Könnicke: *ATM*, Vol. 91 (1939), T-2-4.
- (19) A.L. Jorissen and H.T. Newton: *Trans. ASME*, Vol. 74, No. 5 (1952), p. 825.
- (20) M. Maekawa: *Trans. Japan Soc. Mech. Engrs.*, Vol. 3, No. 12 (1937), p. 244.
- (21) L. Schiller: *Z.AMM*, Bd. 2, Ht. 2 (1922), S. 96.
- (22) S. Goldstein: *Modern Developments in Fluid Dynamics*, Vol. 1 (1938), p. 307, Oxford University Press.
- (23) Y. Nakayama and H. Endo: *Bulletin of JSME*, Vol. 2, No. 6 (1959), p. 212.
- (24) S. Iwanami: Material for 120 Course (May 28, 1959) p. 85, Japan Soc. Mech. Engrs.